

# Climate Change Impacts on Hydropower Management

Ludovic Gaudard · Manfred Gilli · Franco Romerio

Received: 6 July 2013 / Accepted: 7 October 2013 / Published online: 26 October 2013  
© Springer Science+Business Media Dordrecht 2013

**Abstract** Climate change affects hydropower production by modifying total annual inflow volumes and their seasonal distribution. Moreover, increasing air temperatures impact electricity consumption and, as a consequence, electricity prices. All together, these phenomena may lead to a loss in revenue. We show that an adequate management of hydropower plants mitigates these losses. These results are obtained by resorting to an interdisciplinary approach integrating hydrology, economy and hydropower management in an interdependent quantitative model.

**Keywords** Climate change · Hydropower management · Electricity market · Switzerland

## 1 Introduction

Electricity companies need to adapt their strategies in relation to various changes. The most challenging are climate change, liberalization of the electricity market and, for some countries, phase-out of nuclear power. With its flexibility and capacity for storing energy, hydropower may be essential to perform a successful transition as well as being a pillar for the future European electricity market. That is why any impact on the resource may be of high importance.

---

L. Gaudard (✉)  
Institute for Environmental Sciences, University of Geneva,  
Route de Drize 7, 1227 Carouge, Switzerland  
e-mail: ludovic.gaudard@unige.ch

M. Gilli · F. Romerio  
University of Geneva, Bd du Pont d'Arve 40, 1211 Geneva, Switzerland

M. Gilli  
e-mail: Manfred.Gilli@unige.ch

F. Romerio  
e-mail: Franco.Romerio@unige.ch

Unlike disciplinary studies that address specific problems, an interdisciplinary analysis including hydrology and economy is needed to obtain a complete understanding of the system. Existing literature either investigates the impact of climate change on hydropower generation by means of a hydrological model (Hänggi and Weingartner 2012; Finger et al. 2012) or focuses on the impact of global warming on the electricity market (Ahmed et al. 2012; Christenson et al. 2006; Golombek et al. 2012). To our knowledge, no investigation so far, considers the impacts on runoff and economy (energy prices) in an interdependent setting applied to a real hydro power plant. Following Hänggi and Weingartner (2012), “Most of the hydrological studies have analyzed changes to naturally available runoff quantities in isolation; their results frequently do not address issues of water management”. This research is an attempt to fill this gap by providing a quantitative approach combining models from climatology, hydrology, econometrics and operational research.

The paper is organized as follows: Section 2 starts with a general description of the modeling framework and in the following details the components of model, i.e. hydrological evolution, impact of higher air temperature on energy demand, electricity demand and prices, scenarios for future prices and finally the optimization process. In Section 3 the simulation results for the long term evolution and the seasonal changes are discussed. Section 4 concludes.

## 2 The Model

The model connects phenomena induced by the climate change, i.e. hydrology, warming, energy demand and energy prices evolution, to hydropower management, i.e. the amount of processed water. Given exogenous air temperature and runoff forecasts, we model future energy demand and prices and compute an optimal turbine schedule for 2011–2100 in terms of revenue. In order to take account of the variability of future inflows and energy prices a set of results is computed by means of extensive simulations.

Our aim is to come up with an efficient management of the turbine schedule. This is not a trivial problem due to the interaction of inflows, technical constraints and electricity prices, the more as our modeling period runs over 120 years.

Figure 1 illustrates the different components of the overall framework. On top we have the elements which are exogenous in our model, i.e. climate, runoff and air temperatures. Water inflow will change in relation to climate change and glacier retreat while the increasing air temperature impacts electricity prices. They are linked to the demand, driven by heating and cooling degree days (*HDD* and *CDD*), which in turn are defined from the air temperatures. We provide a model for forecasting *HDD* and *CDD*. Electricity prices and runoff are then the main determinants for the management of the plant.

### 2.1 Field Site

Our model is tested on Mauvoisin installations (7°35' E, 46°00' N), located in the southern part of Switzerland. The facilities are supplied by water coming from a sub-catchment of the Rhone River. Areas of natural and derived watersheds measure

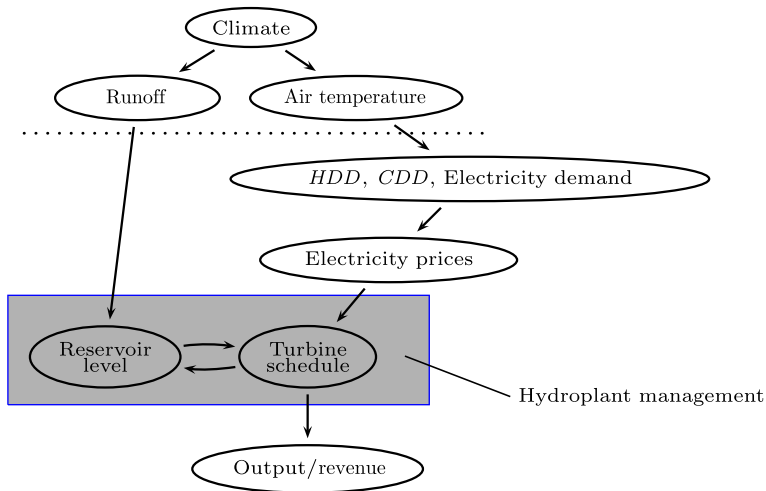


**Fig. 1** Overall modeling framework

114 km<sup>2</sup> and 53 km<sup>2</sup> respectively. Altitude ranges from 1838 to 4321 m a.s.l. At present, glaciers cover 40 % of the basin area.

The installation belongs to Force Motrice de Mauvoisin S.A. (FMM), which owns the water rights until 2041. The installation includes three power plants, one dam and one compensating basin. The main reservoir has a volume of  $192 \times 10^6$  m<sup>3</sup> corresponding to 624 GWh. The present mean annual electricity production is 1040 GWh. The two power plants Fionnay and Riddes are operated as coupled storage power plants. A run-of-river power plant, named Chanrion, is located upstream the Mauvoisin reservoir.

## 2.2 Components of the Model

In the following, we detail the different components of the modeling framework and explain their connections.

### 2.2.1 Runoff

Various modeling studies have been conducted to quantify the runoff to the Mauvoisin reservoir (Terrier et al. 2011; Schaeffli et al. 2007). The most recent one is the analysis carried out by Gabbi et al. (2012), who provide daily runoff estimations based on the GERM model (Farinotti et al. 2012; Huss et al. 2008). They consider ten regional climate models<sup>1</sup> (RCM) from the ENSEMBLES project,<sup>2</sup> all based on the A1B CO<sub>2</sub> emission scenario of the Intergovernmental Panel on Climate Change<sup>3</sup>

<sup>1</sup>List of RCMs considered: ETHZ\_HadCM3Q0\_CLM, HC\_HadCM3Q0\_HadRM3Q0, SMHI\_HadCM3Q3\_RCA, SMHI\_ECHAM\_RCA, MPI\_ECHAM\_REMO, KNMI\_ECHAM\_RACMO, ICTP\_ECHAM\_REGCM, DMI\_ECHAM\_HIRHAM, CNRM\_ARPEGE\_ALADIN, SMHI\_BCM\_RCA

<sup>2</sup>[ensembles-eu.metoffice.com](http://ensembles-eu.metoffice.com)

<sup>3</sup>[www.ipcc.ch](http://www.ipcc.ch)

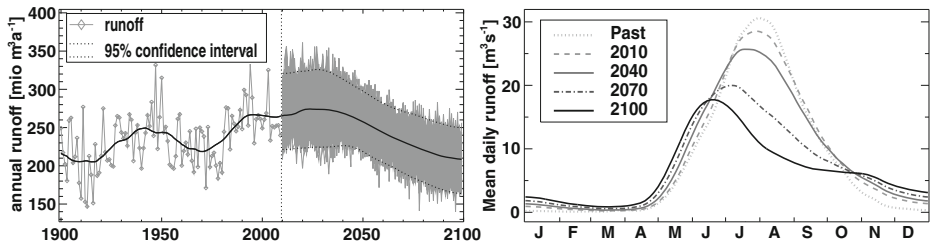


**Fig. 2** *Left panel:* Evolution of runoff to the Mauvoisin reservoir from 1900 to 2100 with confidence interval for forecasted values. *Right panel:* Evolution of annual runoff regime (Gabbi et al. 2012)

(IPCC). Their results suggest that the runoff to the Mauvoisin reservoir will first increase and then wane from 2030–2040. Initially, glacier melt will increase the water inflow to the reservoir, but in the following, it will decrease due to the loss on ice stock. Compared to 2001–2010 the loss will be 18 % by 2091–2100. In addition, climate change will affect the monthly inflow distribution, i.e. flow will increase during spring and autumn and decrease during summer. This evolution is illustrated in Fig. 2 and is used in our model.

### 2.2.2 Heating and Cooling Degree Days (*HDD*, *CDD*)

The consumption of energy is driven by the air temperature. Its impact is measured indirectly by considering so called heating degree days (*HDD*) and cooling degree days (*CDD*). For our purpose the time series of *HDD* and *CDD* are defined as

$$HDD_t = \sum_{i_{\text{Stat}}=1}^{n_{\text{Stat}}} \omega_{i_{\text{Stat}}} \max(\tau_H - \theta_{i_{\text{Stat}}t}, 0) \quad (1)$$

$$CDD_t = \sum_{i_{\text{Stat}}=1}^{n_{\text{Stat}}} \omega_{i_{\text{Stat}}} \max(\theta_{i_{\text{Stat}}t} - \tau_C, 0) \quad (2)$$

where  $\theta_{i_{\text{Stat}}t}$  is the air temperature<sup>4</sup> at weather station  $i_{\text{Stat}}$  at time  $t$  and  $\tau_H = 13^\circ \text{C}$  is the threshold which triggers additional electricity consumption for heating and  $\tau_C = 18.3^\circ \text{C}$  the corresponding term for cooling. Each measurement is weighted by  $\omega_{i_{\text{Stat}}}$  which corresponds to the proportion of the population in the area of weather station  $i_{\text{Stat}}$ .

Figure 3 shows the location of the  $n_{\text{Stat}} = 52$  weather stations used for the computation of *HDD* and *CDD*. Their respective weight is represented by the size of the circles.

In order to evaluate the impact of global warming on electricity consumption and prices, we forecast *HDD* and *CDD*. This requires knowledge about the evolution of air temperatures at the location of the weather stations. To compute this evolution we resort to the ten regional climate models (RCM) from the ENSEMBLES project. These models cover Switzerland with a grid resolution of 25 km. For each weather

<sup>4</sup>Historical air temperatures are provided by MeteoSuisse.

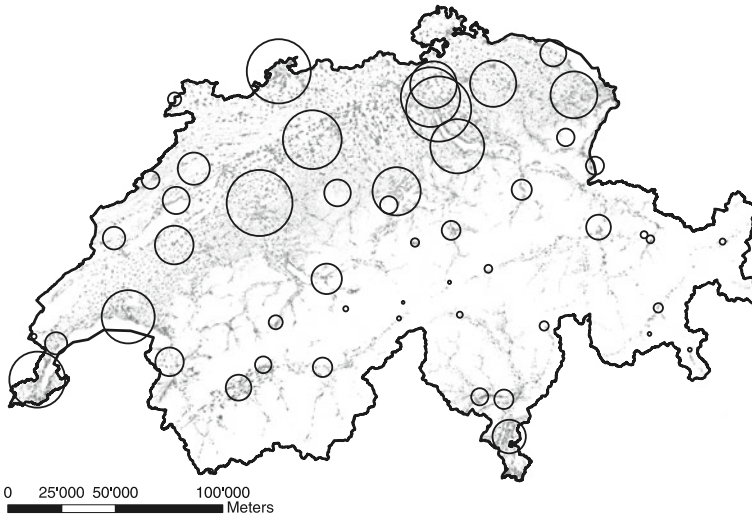


**Fig. 3** Location of  $n_{\text{Stat}} = 52$  weather stations and their respective weight  $\omega_{i_{\text{Stat}}}$  (size of circles) for the computation of *HDD* and *CDD*

station we use the RCM air temperature forecast of the nearest grid point. The procedure builds on the so-called Delta method (Keller et al. 2005; Uhlmann et al. 2009), but in our approach we consider the complete empirical distribution of air temperatures instead of deciles as done in the cited paper. The procedure is summarized in Algorithm 1 for a given climate model. The symbol  $F$  denotes empirical distributions of air temperatures, the indices refer to periods and locations and  $P$  designates grid points of the RCM.

---

#### Algorithm 1 Forecasting HDD and CDD

---

- 1: For a given climate model RCM
  - 2: **for**  $i_{\text{Stat}} = 1 : n_{\text{Stat}}$  (all weather stations) **do**
  - 3: Find  $P_{i_{\text{Stat}}}$  (nearest grid point of RCM to weather station  $i_{\text{Stat}}$ )
  - 4: **for**  $i_{\text{Month}} = 1 : 12$  (each month over a period of 30 years) **do**
  - 5: Compute  $F_{i_{\text{Stat}}}^{1981--2010, i_{\text{Month}}}$  (at weather station  $i_{\text{Stat}}$ )
  - 6: Save  $I_{\text{Orig}}$  (original order of air temperatures)
  - 7: Compute  $F_{P_{i_{\text{Stat}}}}^{1981--2010, i_{\text{Month}}}$  (at grid point  $P_{i_{\text{Stat}}}$ )
  - 8: **for**  $i_{\text{Period}} = 1 : 3$  (periods: 2011–2040, 2041–2070 and 2071–2100) **do**
  - 9: Compute  $F_{P_{i_{\text{Stat}}}}^{i_{\text{Period}}, i_{\text{Month}}}$
  - 10: Compute  $\Delta = F_{P_{i_{\text{Stat}}}}^{i_{\text{Period}}, i_{\text{Month}}} - F_{P_{i_{\text{Stat}}}}^{1981--2010, i_{\text{Month}}}$
  - 11: Compute  $F_{i_{\text{Stat}}}^{i_{\text{Period}}, i_{\text{Month}}} = \Delta + F_{i_{\text{Stat}}}^{1981--2010, i_{\text{Month}}}$
  - 12: Sort air temperatures according to  $I_{\text{Orig}}$
  - 13: **end for**
  - 14: **end for**
  - 15: Assemble air temperatures into a daily time series of 90 years
  - 16: **end for**
  - 17: Compute *HDD* and *CDD* with the  $n_{\text{nStat}}$  air temperature time series
-

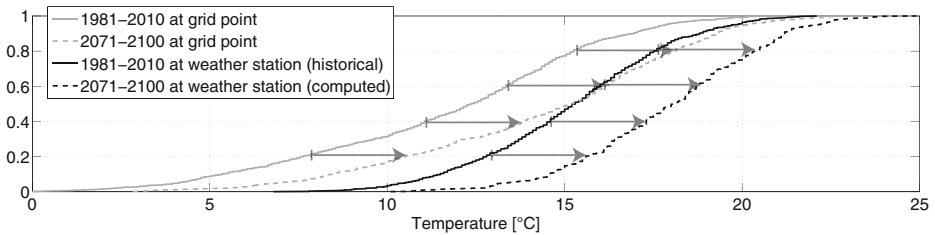


**Fig. 4** Illustration of  $\Delta$  method for period 2071–2100 and month September at weather station Sion

The  $\Delta$  method adapts the climate model forecasts to the profile of the historical data measured at the weather station. Indeed the method not only considers the increase of air temperatures, but also models the modifications of the annual air temperature variability. This is illustrated in Fig. 4 where the arrows correspond to the computed  $\Delta$  (for each point in the empirical distribution). In summary, the air temperature forecasts at a given weather station is obtained by shifting its historical distribution by  $\Delta$ , i.e. the difference between observed and forecasted air temperature distributions at its nearest grid point.

The air temperature distribution for the complete period 2071–2100 for the same weather station (Sion) is illustrated in Fig. 5.

One may ask why not simply resort to the air temperature forecasts at the grid points? One reason is that the environmental conditions at the grid point are generally different from those at the weather station, as they do not overlap. For example, in Fig. 5, we observe a maximum gap of about 10 °C around the median of the distributions, this because the weather station is situated at a lower altitude than the grid point. Another reason is that the observed air temperatures at the weather stations add information to a relatively coarse regional climate models.

Given the forecasted air temperatures we can compute the *HDD* and *CDD* defined by the Eqs. 1 and 2. Figure 6 shows the evolution of the seasonal *HDD* and *CDD* for 2071–2100 and compares them to the ones observed for 1981–2010.

Due to increasing air temperatures, *HDD* and *CDD* will change over coming decades. Comparing 1981–2010 to 2071–2100 (cf. Fig. 6), *HDD* decreases by an average of 29 %, within an interval of 20–37 %, depending on the RCM. Meanwhile, *CDD* grows by a factor of about 3.2, within an interval of 2.1–4.2. As a consequence

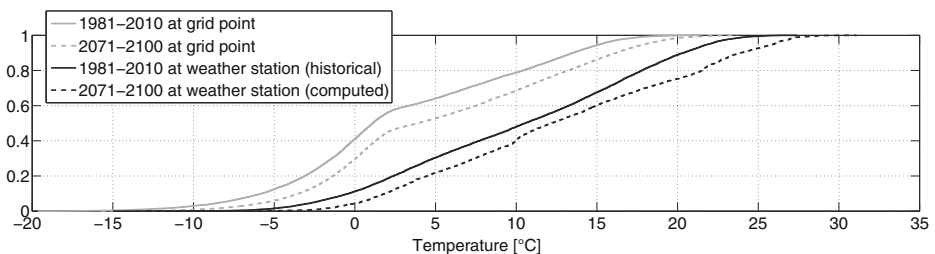


**Fig. 5** Empirical distribution of forecasted air temperatures for 2071–2100 at weather station Sion

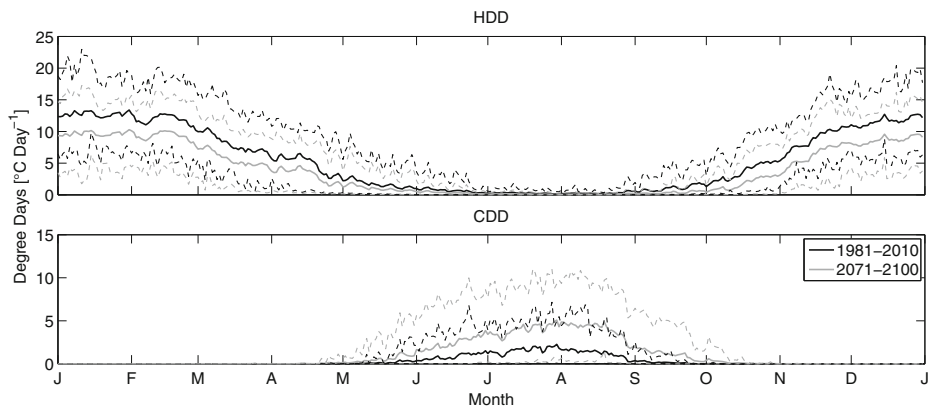


**Fig. 6** Evolution of forecasted seasonal *HDD* and *CDD* for 2071–2100 and observed values for 1981–2010. Solid lines represent means and dotted lines represent confidence intervals (5 and 95 quantiles)

the future mean values for *CDD* will reach those of the upper 95 quantile of the historical period 1981–2010. This issue has already been emphasized in a study concerning four major cities in Switzerland (Christenson et al. 2006). Note however, that these results are not directly comparable as our forecasts consider the whole country and are built on different definitions of *HDD* and *CDD*.

### 2.2.3 Energy Consumption and Prices

The relation between daily electricity consumption and *HDD*, *CDD* is modeled with a log-log model as:

$$\log(C_t) = \alpha_0 + \alpha_1 \log(HDD_t + 1) + \alpha_2 \log(CDD_t + 1) + \alpha_3 D_t^{\text{Sat}} + \alpha_4 D_t^{\text{Sun}} + \alpha_5 D_t^{\text{Hol}} + \epsilon_t \quad (3)$$

where  $C_t$  is the daily consumption and  $D_t^{\text{Sat}}$ ,  $D_t^{\text{Sun}}$ ,  $D_t^{\text{Hol}}$  are dummy variables for Saturday, Sunday and holidays. These latter are variables taking the value 0 or 1. Negative values for the logarithms are avoided by adding a unit shift.

Given the consumption prices we are able to model hourly electricity spot prices as a function of daily consumption and a set of dummy variables characterizing sub-day variations as:

$$\log(P_t^h) = \beta_0 + \beta_1 C_t + \sum_{i=2}^3 \beta_i D_t^{\text{day}_i} + \sum_{i=4}^{25} \beta_i D_t^{\text{hour}_i} + \delta_t \quad (4)$$

where  $P_t^h$  is the hourly spot price,  $D_t^{\text{day}_i}$  are the dummy variables for Saturday and Sunday,  $D_t^{\text{hour}_i}$  the dummy variables for the hours of the day. They start with  $\text{hour}_4$  for the time interval going from 1 to 2 a.m., do not include the time interval from 8 to 9 a.m. (as this interval is not significant in the regression) and end with  $\text{hour}_{25}$  corresponding to the last hour of the day. The error term  $\delta_t$  follows a combined ARMA(1, 1), GARCH(1, 1) model.

**Table 1** Values for the significant parameters in the consumption Eq. 3

$\alpha_0$	$\alpha_1$	$\alpha_2$	$\alpha_3$	$\alpha_4$	$\alpha_5$
5.03	0.10	0.04	-0.14	-0.20	-0.22

Tables 1 and 2 summarize the estimation results for the Eqs. 3 and 4. Consumption data have been provided by Swissgrid and the electricity prices for Switzerland are provided by European Energy Exchange (EEX). The observations cover the period going from 2009 to 2011.

#### 2.2.4 Hydropower Plant Management

According to the forecasted prices we determine the management of the power plant. The hydropower plant's input is water inflow and its output is electrical energy, which has a market price. The objective function, which defines the management, is given by the revenue corresponding to the produced energy plus the value of the residual volume of water in the reservoir. The management is constrained by the capacity of the reservoir as well as inflow and turbine capacity. Thus the objective function writes:

$$OF(z) = g \rho \eta f \Delta_t \left( \sum_{t=1}^{t=T} h_t z_t P_t \right) + R_T \quad (5)$$

where the physical and technical constants are: acceleration due to gravity  $g$ , water density  $\rho$ , plant efficiency  $\eta$  and  $f$  water flow through the turbine.  $\Delta_t$  is the unit time interval of operation (1 hour in our analysis). The time horizon for the optimization is  $T$ ,  $h_t$  is the hydraulic head,  $P_t$  is the electricity spot price and  $z_t$  is a binary variable indicating whether production is on or off.  $R_T$  is the value of the residual volume of water in the reservoir, i.e. at the end of the optimization period. The residual value  $R_T$  is defined as the virtual revenue produced as if the complete residual water would have been processed following the end of the 2 years of the optimization window. It is approximated by taking the computed turbine schedule and the corresponding

**Table 2** Values for the significant parameters in the electricity price Eq. 4

						Sat		Sun			
		$\beta_0$		$\beta_1$		$\beta_2$		$\beta_3$			
		-33		0.48		5.40		2.18			
hours	1-2	2-3	3-4	4-5	5-6	6-7	7-8	9-10	10-11	11-12	12-13
	$\beta_4$	$\beta_5$	$\beta_6$	$\beta_7$	$\beta_8$	$\beta_9$	$\beta_{10}$	$\beta_{11}$	$\beta_{12}$	$\beta_{13}$	$\beta_{14}$
	-6.72	-11.98	-16.37	-19.46	-20.32	-14.34	-5.26	-6.65	-9.21	-10.29	-11.65
hours	13-14	14-15	15-16	16-17	17-18	18-19	19-20	20-21	21-22	22-23	23-24
	$\beta_{15}$	$\beta_{16}$	$\beta_{17}$	$\beta_{18}$	$\beta_{19}$	$\beta_{20}$	$\beta_{21}$	$\beta_{22}$	$\beta_{23}$	$\beta_{24}$	$\beta_{25}$
	8.52	6.65	5.91	4.78	4.73	6.84	9.38	8.87	7.24	5.15	4.34



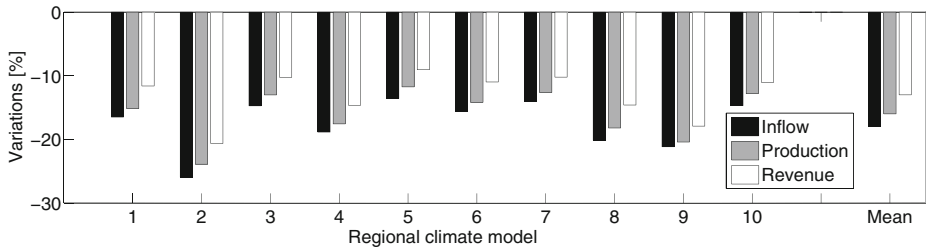


**Fig. 7** Forecasted variations of inflow, production and revenue from 2001–2010 to 2091–2100 for all regional climate models (in the order given in footnote 1)

prices until exhaustion of the water. In the case of our plant we have  $\eta = 0.85$  and  $f = 34.5 \text{ m}^3/\text{s}$ . The optimization problem is then formulated as:

$$\begin{aligned}
 & \max_z OF(z) \\
 & V_t = V_{t-1} + I_t \Delta_t - f z_t \Delta_t \\
 & h_t = \Phi(V_t) \\
 & V_{\min} < V_t < V_{\max} \\
 & z_t \in \{0, 1\}
 \end{aligned}$$

where  $V_t$  is the current reservoir content,  $I_t$  the water intake,  $h_t$  is determined as function of  $V_t$  and  $V_{\min} = 0$ ,  $V_{\max} = 192 \times 10^6 \text{ m}^3$  are the capacity limits of the reservoir.

The problem has been solved using a local search heuristic called Threshold Accepting<sup>5</sup> (Dueck and Scheuer 1990; Moscato and Fontanari 1990). As the optimization runs over 120 years we considered a window of 2 years, sliding forward year by year and keeping the results of the first half of the window. This results into a sequence of 120 optimization problems where the dimension of variable  $z$  is  $T = 8760 \times 2 = 17520$ .

### 3 Simulations

We analyze the impact of climate change on the generation of revenue and the management of the power plant as consequence of modified inflows and electricity consumption. Figure 7 shows the forecasted variations in inflow, production and revenue for the storage plant from 2001–2010 to 2091–2100 for the different regional climate models, as well as the overall mean, corresponding to the base scenario specified below.

The models forecast that inflows are expected to decrease at average by 18 % from 2001–2010 to 2091–2100 (Fig. 7). In consequence one might expect a similar drop in production and revenue which, however, is not the case for the results in the Figure. Indeed our investigations show that adequate management can mitigate the loss,

<sup>5</sup>For implementation details see Gilli et al. (2011).

(i) in hydro power by optimizing the hydraulic head, (ii) in revenue by optimizing the turbine schedule with respect to the prices.

First, the power loss due to reduced inflows and the corresponding lowering of the hydraulic head amounts to some 20 %. But maximizing the hydraulic head of the reduced volume, diminishes this loss to 16 %. Second, the optimal turbine schedule partially compensates the power losses by an additional revenue of 3 %. Therefore, the overall loss in revenue is only in the order of 13 %.

In the following we discuss the evolution of these quantities as well as the seasonal changes. Impacts on consumption have been modeled according to two different assumptions.

### 3.1 Price Scenarios

Our analysis concentrates on climate change impacts and the following consumption and price scenarios are not meant as economic forecasts but rather serve sensitivity investigations.

Air temperatures define *HDD* and *CDD* which in turn enter the consumption equation and then explains prices. Given a base scenario where *HDD* and *CDD* remain at the levels observed for the historical period 1981–2010 we investigate two situations, both with the forecasted *HDD* and *CDD*:

- A) Consumption evolves according to Eq. 3 as estimated;
- B) Consumption behavior is modified by setting  $\alpha_1 = \alpha_2 = 0.09$ . We assume the same reaction of consumption with respect to changes in *HDD* and *CDD*.

Scenario B translates current trends in consumption, i.e. reduced reactivity to *HDD*, due to improved efficiency of heating devices and increasing reactivity to *CDD* as a consequence of a growing number of cooling devices. Moreover the value  $\alpha = 0.09$  has been chosen in a way to get similar annual consumptions for 1981–2010, whether computed with the original or modified coefficients.

It is noteworthy to emphasize that the evolution of consumer behavior expressed in scenario B has higher impact on energy consumption than the increasing temperatures. Indeed, with respect to the base scenario, the daily demand of mid-July increases by about 2 % at the end of the century in scenario A and by about 13 % in scenario B, cf. Fig. 8.

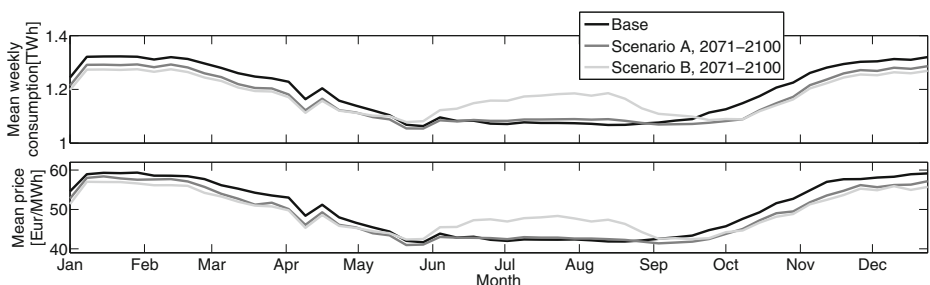


**Fig. 8** Seasonal consumptions and prices according to base scenario and scenarios A and B

### 3.2 Storage Hydropower

The operator manages the production by tracking price fluctuations. The reservoir is filled during summer when inflow is large and emptied during winter when the prices are high. In the long run the simulations show that, the production will, compared to a reference period of 2001–2010, grow by 4 % for the period 2041–2050 and decrease by 16 % for the period 2091–2100 in all scenarios. The revenue follows this same trend. At the end of the century we observe that revenue declines in all scenarios in a range of 13 to 16 %. The highest drop is observed for scenario A.

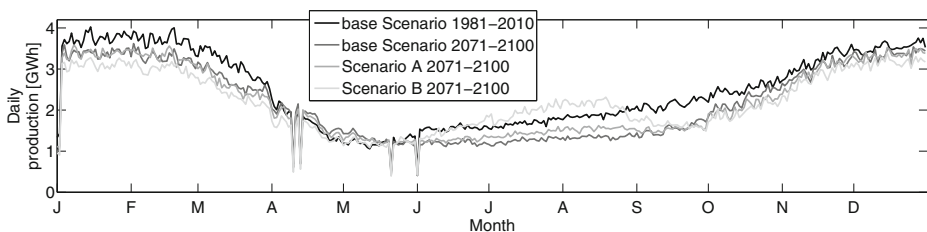
Figure 9 shows the seasonal production for (i) the base scenario for 1981–2010 and 2071–2100 which translates the impact of changes in inflow, (ii) scenarios A and B for 2071–2100 which illustrate the impact of different consumption behaviors.

One might have expected that the future changes in inflow will essentially affect production during the summer season, however our simulations show that production will decrease throughout the whole year, except, perhaps, off season. This might be due to the fact that already at present the constraints in terms of reservoir volume are not very stringent, i.e. the reservoir is oversized for the actual inflow. The five down spikes in the production correspond to the major holidays.

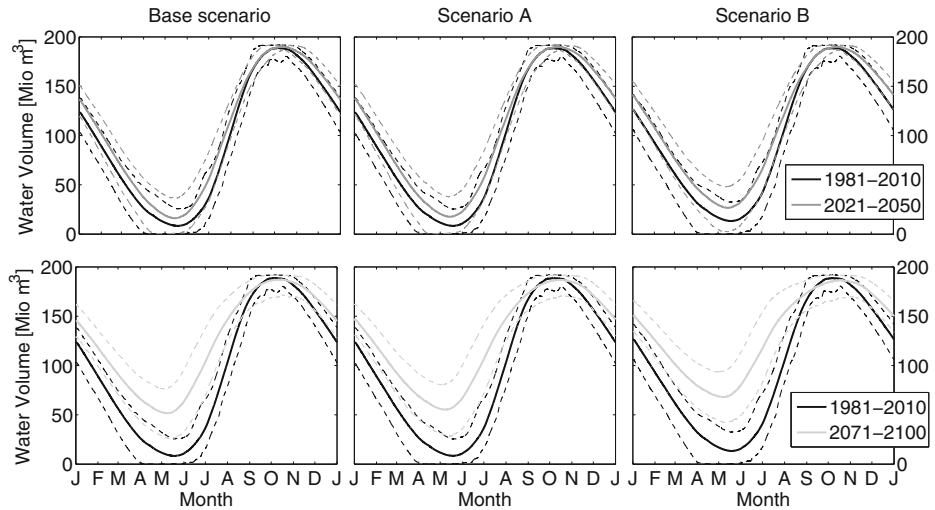
Comparing the production at the end of the century for the three scenarios, we observe little difference between the base and scenario A. For scenario B we see a shift of the production from winter to summer season. This is a consequence of the evolution of prices which increase during summer and decrease in the winter (cf. Fig. 4).

Figure 10 focuses on changes in water volume in the reservoir for mid term 2021–2050 (upper panels) and long term 2071–2100 (lower panels) for the three scenarios. The change in the management of the reservoir we can observe is (i) filling starts earlier, (ii) the minimum water level increases over the years. This is due to the growing deficit of inflow during summer (cf. Fig. 2). Again, the phenomena are more marked for scenario B. We can conclude that the plant design is no longer optimal in this modified environment.

One may expect that the reservoir should rather become emptier, as inflow decreases. The reason for the increase of the reservoir level is that our optimization takes into account the hydraulic head, i.e. a higher head results in more power output. In our optimal management we raise the mean level of the reservoir by keeping a fixed volume of water throughout the year.



**Fig. 9** Seasonal production for base scenario for periods 1981–2010, 2071–2100 and scenarios A and B for 2071–2100



**Fig. 10** Seasonal reservoir water volume for periods 1981–2010, 2021–2050 (*upper panels*) and 1981–2010, 2071–2100 (*lower panels*) for all three scenarios. *Solid lines* represent means and *dotted lines* represent confidence intervals (5 and 95 quantiles)

The 5 and 95 quantile intervals have been computed from 60 simulations, corresponding to ten different climate models (RCM), each model ran with six different hydrological forecasts. These simulations span over the 30 years of a period. These time series are then split into 30 yearly series which then results into 1800 yearly profiles.

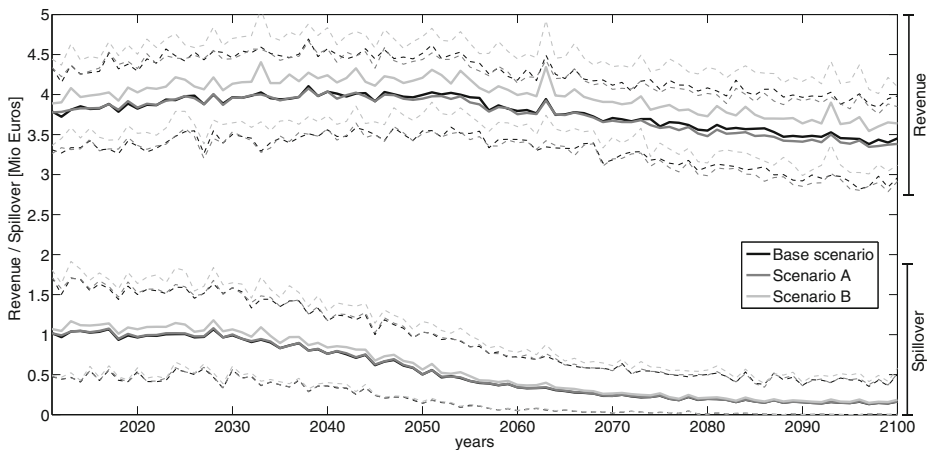


**Fig. 11** Annual revenues (*upper lines*) and spillovers (*lower lines*) for the run-of-river plant over the entire modeling horizon. The 5 and 95 quantile intervals (*dotted lines*) are obtained from  $10 \times 6 = 60$  time series running over the whole period

### 3.3 Run-of-river Hydropower

Unlike storage hydropower plants, run-of-river production is not linked to electricity prices but only to seasonal variations of inflows and therefore revenue is affected only by pipeline capacity, which in our case is  $10 \text{ m}^3/\text{s}$ . As a consequence management does not require any optimization.

Two phenomena are discussed in Fig. 11. In the upper part of the Figure, the evolution of the yearly revenue for the entire modeling horizon is traced. We observe two regimes, for the first half of the period, revenue is slightly increasing while for the second half we observe a decline of about 10 %. There is no difference between base scenario and scenario A. However for scenario B revenues are about 5 % higher, due to the higher electricity prices during summer.

The lower part of Fig. 11 displays the evolution of the spillover due to the pipeline constraint. Its market value is computed as if the water was exploited by the turbine. As expected spillover diminishes as inflow decreases over time. This also explains why we observe a very small change in revenue.

## 4 Conclusions

As a consequence of climate change inflows are expected to decrease and as a consequence one might expect similar drops in production and revenue. However, our results show that adequate management mitigates these losses. Indeed the losses of energy production and revenue can be partially compensated by optimizing the hydraulic head and the turbine schedule. These results highlight the interest of a global modeling framework adapting management to the changing hydrological environment in opposition to research where reservoir management is independent to changes in the runoff regime.

Our results have been established on a set of sixty hydrological simulations based on ten regional climate models all covering the period from 1981 to 2100.

The results, based on *HDD* and *CDD*, also show that there will be little impact of climate change on electricity demand. Scenario B suggests, that changes in consumer behavior may play a more important role with respect to demand, particularly resulting in increased production during the summer season.

Finally, the outcomes may be helpful, in particular, in the decision process for future hydropower investments, and more generally for the future energy policy favoring renewable energies. The increasing unused reservoir capacities could be used to regulate the intermittency of renewable energies by means of pumping systems. We are currently investigating these issues.

**Acknowledgements** This study was carried out within the frame of the Swiss research programme 61 ([www.nfp61.ch](http://www.nfp61.ch)). We are grateful to the Versuchsanstalt für Wasserbau, Hydrologie und Glaziologie, in particular, Martin Funk, Andreas Bauder and Jeannette Gabbi for providing hydrological data and essential information. We also thank Force Motrices de Mauvoisin for the reservoir management data and sharing their expertise. The ENSEMBLES data used in this work was funded by the EU FP6 Integrated Project ENSEMBLES (Contract number 505539). Martin Beniston and Stephan Goyette provided valuable scientific input and Christophe Etienne and Denis Cohen proofread an earlier version of the paper.

## References

- Ahmed T, Muttaqi KM, Agalgaonkar AP (2012) Climate change impacts on electricity demand in the State of New South Wales, Australia. *Appl Energy* 98:376–383
- Christenson M, Manz H, Gyalistras D (2006) Climate warming impact on degree-days and building energy demand in Switzerland. *Energy Convers Manag* 47(6):671–686
- Dueck G, Tobias S (1990) Threshold accepting. A general purpose optimization algorithm superior to simulated annealing. *J Comput Phys* 90(1):161–175
- Farinotti D, Usselmann S, Huss M, Bauder A, Funk M (2012) Runoff evolution in the Swiss Alps: projections for selected high-alpine catchments based on ensembles scenarios. *Hydrol Process* 26(13):1909–1924
- Finger D, Heinrich G, Gobiet A, Bauder A (2012) Projections of future water resources and their uncertainty in a glacierized catchment in the Swiss Alps and the subsequent effects on hydropower production during the 21st century. *Water Resour Res* 48. doi:10.1029/2011WR010733
- Gabbi J, Farinotti D, Bauder A, Maurer H (2012) Ice volume distribution and implications on runoff projections in a glacierized catchment. *Hydrology Earth Syst Sci* 16(12):4543–4556
- Gilli M, Maringer D, Schumann E (2011) Numerical methods and optimization in finance. Elsevier
- Golombek R, Kittelsen SAC, Haddeland I (2012) Climate change: impacts on electricity markets in Western Europe. *Clim Chang* 113(2):357–370
- Hänggi P, Weingartner R (2012) Variations in discharge volumes for hydropower generation in Switzerland. *Water Resour Manag* 26(5):1231–1252
- Huss M, Farinotti D, Bauder A, Funk M (2008) Modelling runoff from highly glacierized alpine drainage basins in a changing climate. *Hydrol Process* 22(19):3888–3902
- Keller F, Goyette S, Beniston M (2005) Sensitivity analysis of snow cover to climate change scenarios and their impact on plant habitats in alpine terrain. *Clim Chang* 72(3):299–319
- Moscato P, Fontanari JF (1990) Stochastic versus deterministic update in simulated annealing. *Phys Lett A* 146(4):204–208
- Schaeffli B, Hingray B, Musy A (2007) Climate change and hydropower production in the Swiss Alps: quantification of potential impacts and related modelling uncertainties. *Hydrol Earth Syst Sci* 11(3):1191–1205
- Terrier S, Jordan F, Schleiss AJ, Haeberli W, Huggel C, Künzler M (2011). Optimized and adapted hydropower management considering glacier shrinkage scenarios in the Swiss Alps. In: Schleiss A J, Boes R M (eds) *Dams and reservoirs under changing challenges*. Leiden, pp. 497–508
- Uhlmann B, Goyette S, Beniston M (2009) Sensitivity analysis of snow patterns in Swiss ski resorts to shifts in temperature, precipitation and humidity under conditions of climate change. *Int J Climatol* 29(8):1048–1055